ISSN 1064-2269, Journal of Communications Technology and Electronics, 2014, Vol. 59, No. 5, pp. 441–455. © Pleiades Publishing, Inc., 2014.
Original Russian Text © V.S. Vlasov, V.G. Shavrov, V.I. Shcheglov, 2014, published in Radiotekhnika i Elektronika, 2014, Vol. 59, No. 5, pp. 482–497.

RADIO PHENOMENA IN SOLIDS AND PLASMA

Nonlinear Excitation of Ultrasound in a Two-Layer Ferrite Structure under Ferromagnetic Resonance Conditions

V. S. Vlasov[a], V. G. Shavrov[b], and V. I. Shcheglov[b]

[a] *Syktyvkar State University, Syktyvkar, Oktyabr'skii pr. 55, 167001 Russia*

[b] *Kotel'nikov Institute of Radio Engineering and Electronics, Russian Academy of Sciences, Mokhovaya ul. 11, korp. 7, Moscow, 125009 Russia*

e-mail: vshcheg@mail.cplire.ru

Received April 10, 2013

Abstract—The nonlinear problem of excitation of hypersound in a normally magnetized structure is considered. The structure consists of two ferrite layers, its elastic properties are constant across the entire structure thickness, and the magnetic properties of the layers can be different. The equations of motion and boundary conditions for the magnetization components and elastic displacement are obtained for the case of an arbitrary angle of the magnetization vector precession. Using the decomposition in eigenmodes, the problem is reduced to a system of an infinite number of second-order differential equations. In the case when the first elastic mode is excited, the complete problem is reduced to a system of thirty nonlinear first-order differential equations solved numerically by means of the Runge–Kutta method. The time evolution and amplitude–frequency characteristics of excited oscillations are considered. Conditions under which the amplitude of nonlinear-mode elastic vibrations exceeds the amplitude of linear-mode elastic vibrations by a factor as large as 70 and the bandwidth increases by a factor as large as five are revealed.

DOI: 10.1134/S1064226914040135

INTRODUCTION

Excitation of ultrasonic vibrations with the help of magnetostrictors [1–4] is widely applied in hydroacoustics, defectoscopy, ultrasound processing, medical equipment, and other fields. Vibrations at comparatively low frequencies (not exceeding hundreds of kilohertz) are usually used. The application of magnetostrictors is rather promising in acoustoelectronics, where the high mechanical Q factor of ferrite transducers (which can reach 10^7 with yttrium iron garnet (YIG) employed) enables the development of highly efficient devices for microwave data processing ($f \sim 10^9$–10^{11} Hz).

Even in the first experimental studies devoted to ultrasound excitation with the help of magnetoacoustic transducers based on the ferromagnetic-resonance (FMR) in YIG [5, 6], the high efficiency of excitation combined with the low attenuation of acoustic pulses was revealed. However, it was soon found [4, 7] that the admissible power of the fed signal is limited by a level of about 1 mW, a circumstance related with the parametric decay of the uniform precession and excitation of exchange spin waves [8–11].

On the basis of experimental and theoretical data, it was shown in [12–16] that the parametric decay could be prevented through choosing the geometry of a transducer in the form of a normally magnetized thin disk such that the lowest frequency of its FMR coincided with the bottom of the spectrum of exchange spin waves.

The historically first theory of hypersound excitation with the help of a magnetoacoustic transducer based on a normally magnetized ferrite disk was developed in [3, 4]; however, because of its linear character, the maximum excitation efficiency in the presence of a high-intensity signal could not be estimated.

Certain estimates obtained in [17, 18] were mainly qualitative.

In [20], a nonlinear theory was developed and a quantitative estimate was obtained with the use of data from [12–15]. According to this estimate, the amplitude of hypersound excited in the nonlinear mode can exceed the linear-mode hypersound amplitude by a factor not less than 30. However, the analysis performed in those studies was primarily oriented toward reaching the maximum excitation amplitude and disregarded the frequency spectrum of the excited hypersound. In [21], the authors attempted to solve partly the problem for a double-layer structure; however, the analysis performed in that study was incomplete: only the time evolution of vibrations was obtained, but their properties were not studied and or compared to the properties of vibrations in a single-layer structure.

This study develops the results obtained in [20, 21]. Our main task is to reveal new possibilities of excitation of magnetic oscillations and elastic vibrations in a double-layer structure. These possibilities are due to the different magnetic parameters of the layers forming the structure.

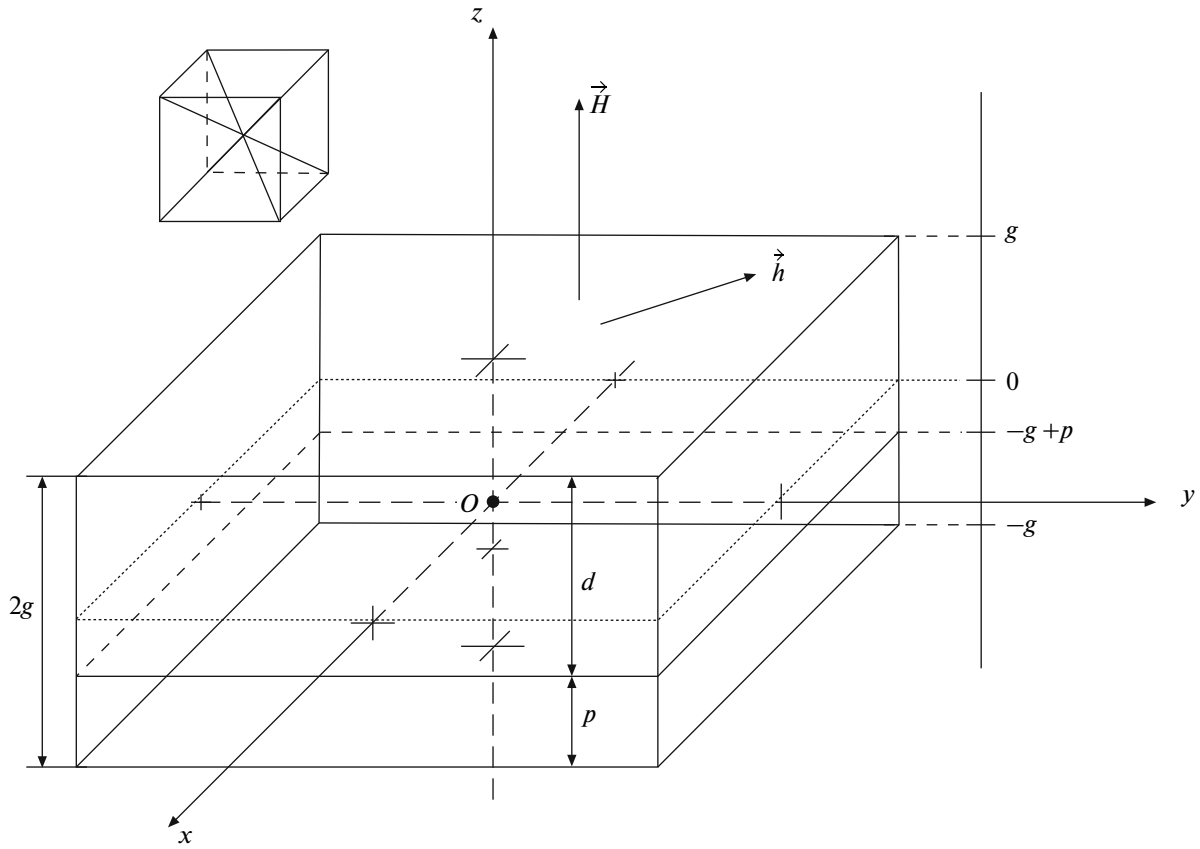

Fig. 1. General geometry of the problem on a double-layer structure.

1. GEOMETRY OF THE PROBLEM AND THE ENERGY DENSITY

The general geometry of the problem is similar to that assumed in [21]. It is displayed in Fig. 1. A double-layer structure consists of two adjacent infinitely extended elastic-ferrite plates. The thicknesses of the first and second layers are p and d, respectively, and the total thickness of the entire structure is $p + d = 2g$. The origin is chosen to be at the center of the entire structure; i.e., the upper and lower surfaces correspond to coordinates g and $-g$, and interface between the layers corresponds to the coordinate $-g + p$. The magnetic and magnetoelastic parameters of the layers are different and, below, are supplied with indices p and d. The elastic parameters of the layers are identical and, therefore, have no indices.

Let us assume that density U of the energy of the structure in the presence of the field $\vec{H} = \{h_x; h_y; H_0\}$ is equal to the sum of the densities of the magnetic, elastic, and magnetoelastic energies of the layers and retain only the constants that are important for the further analysis:

$$\begin{aligned} U &= -M_{p0}h_x m_{px} - M_{p0}h_y m_{py} - M_{p0}H_0 m_{pz} \\ &+ 2\pi M_{p0}^2 m_{pz}^2 + K_{p1}\left(m_{px}^2 m_{py}^2 + m_{py}^2 m_{pz}^2 + m_{pz}^2 m_{px}^2\right) \\ &+ 2c_{44}\left(u_{pxy}^2 + u_{pyz}^2 + u_{pzx}^2\right) + 2B_{p2}(m_{px}m_{py}u_{pxy} \\ &+ m_{py}m_{pz}u_{pyz} + m_{pz}m_{px}u_{pzx}) + U(d), \end{aligned} \quad (1)$$

where H_0 is the external static field, $h_{x,y}$ are the alternate field components, $\vec{m}_{p,d} = \vec{M}_{p,d}/M_{p,d0}$ are the layers' magnetization vectors normalized by corresponding saturation magnetizations $M_{p,d0}$; $u_{p,dik}$ are the components of the deformation tensor $(i, k = x, y, z)$ that correspond to elastic displacements $u_{p,di,k}$; $K_{p,d1}$ are the cubic magnetic anisotropy constants, c_{44} are the elastic constants (identical for both layers), $B_{p,d2}$ are the magnetoelastic interaction constants, and $U(d)$ are analogous terms with index d substituted for index p.

2. BASIC EQUATIONS AND BOUNDARY CONDITIONS

Energy density (1) enables us to obtain for each layer the complete equations of motion for the magnetization and elastic displacement vectors as well as the boundary conditions that express the absence of elastic stresses on the exterior surfaces of the entire structure and the equality of stresses and displacements on the layer interface.

By analogy with [20, 21], we assume that magnetizations $m_{p,d}$ are uniformly distributed inside the layers.

The equations of motion for the magnetization components in layer p have the form

$$\frac{\partial m_{px}}{\partial t} = -\frac{\gamma}{1+\alpha_p^2}\Big[\left(m_{py} + \alpha_p m_{px} m_{pz}\right) H_{pez} - \left(m_{pz} - \alpha_p m_{py} m_{px}\right) H_{pey} - \alpha_p \left(m_{py}^2 + m_{pz}^2\right) H_{pex}\Big], \quad (2)$$

and the equations for m_{py} and m_{pz} can be obtained from (2) via cyclic permutation of x, y, and z. Here, α_p is the attenuation constant and the effective fields are as follows:

$$H_{pex} = h_x + H_{pax}, \quad (3)$$

$$H_{pey} = h_y + H_{pay}, \quad (4)$$

$$H_{pez} = H_0 - 4\pi M_{p0} m_{pz} + H_{paz}, \quad (5)$$

where

$$H_{pax} = -\frac{2K_1}{M_0} m_x \left(m_y^2 + m_z^2\right) - \frac{B_{p2}}{M_{p0}}\left[m_{py}\left(\frac{\partial u_{px}}{\partial y} + \frac{\partial u_{py}}{\partial x}\right) + m_{pz}\left(\frac{\partial u_{pz}}{\partial x} + \frac{\partial u_{px}}{\partial z}\right)\right] \quad (6)$$

and H_{pay} and H_{paz} are obtained via cyclic permutation of x, y, and z.

The equations of motion for the magnetization components in layer d are obtained from (2)–(6) through replacing index p by d.

By analogy with [20, 21], we assume that there are no elastic displacements perpendicular to the plane of the structure, i.e., $u_{p,dz} = 0$, and that displacements $u_{p,dx}$ and $u_{p,dy}$ in the plane of the structure are uniform, i.e., $\partial u_{p,dx,y}/\partial x, y = 0$.

The equation of motion for the x component of the elastic displacement in layer p has the form

$$\frac{\partial^2 u_{px}}{\partial t^2} = -2\delta\frac{\partial u_{px}}{\partial t} + \frac{c_{44}}{\rho}\frac{\partial^2 u_{px}}{\partial z^2}, \quad (7)$$

where δ is the attenuation parameter and ρ is the material density, which is the same for both layers. This is a wave equation that makes it possible to reduce the coordinate dependence to a set of eigenfunctions of the homogeneous problem when the boundary conditions in coordinate z are specified. As a result, the main task becomes the determination of the evolution of the oscillation process in time, a problem that is solved below.

The equation of motion for the y component of the elastic displacement in the same layer p is obtained from (7) through replacing index x by y. By virtue of the above assumptions, there is no equation of motion for the z component. The equations of motion for the same components of the elastic displacement in layer d are similar to (7) with index d substituted for p.

The magnetization is uniform, and, therefore, it is unnecessary to impose boundary conditions for it. The boundary conditions for the x components of the displacements in layers p and d have the form

$$c_{44}\frac{\partial u_{px}}{\partial z} + B_{p2} m_{px} m_{pz}\Big|_{z=-g} = 0 \quad (8)$$

on the lower surface of the structure, at $z = -g$;

$$c_{44}\frac{\partial u_{px}}{\partial z} + B_{p2} m_{px} m_{pz}\Big|_{z=-g+p} = c_{44}\frac{\partial u_{dx}}{\partial z} + B_{d2} m_{dx} m_{dz}\Big|_{z=-g+p}, \quad (9)$$

$$u_{px}\big|_{z=-g+p} = u_{dx}\big|_{z=-g+p} \quad (10)$$

on the interface between the layers, at $z = -g + p$;

$$c_{44}\frac{\partial u_{dx}}{\partial z} + B_{d2} m_{dx} m_{dz}\Big|_{z=g} = 0 \quad (11)$$

on the lower surface of the structure, at $z = g$.

The boundary conditions for the y components of the displacements in the same layers have a form similar to (8)–(11) with index x substituted for y.

Thus, the complete system contains six first-order equations without boundary conditions for the magnetization components and four second–order equations with eight boundary conditions for the elastic displacement components.

We can see that the equations of magnetization oscillations and elastic displacement vibrations in each of the layers are mutually independent and coupled only through boundary conditions (9) and (10). This circumstance enables us to consider the entire problem as a boundary value problem for the elasticity where the magnetizations of the layers are parameters depending only on time.

At the same time, the problems for the x and y components of the elastic displacement (the equation combined with the boundary conditions) in each of the layers are mutually independent; i.e., it suffices to consider only one problem, for example, for the x component. Then, a solution for the y component can be obtained through replacing index x by y. Therefore, below, we consider the problem for both layers in aggregate but only for the x component.

3. THE COMPLETE FORMULATION OF THE PROBLEM FOR THE ELASTICITY

The complete problem for the x component of the elastic displacement in both layers can be represented in the form of the equation (with index x dropped)

$$\frac{\partial^2 u_p}{\partial t^2} + 2\delta\frac{\partial u_p}{\partial t} - \frac{c_{44}}{\rho}\frac{\partial^2 u_p}{\partial z^2} = 0, \quad (12)$$

$$\frac{\partial^2 u_d}{\partial t^2} + 2\delta\frac{\partial u_d}{\partial t} - \frac{c_{44}}{\rho}\frac{\partial^2 u_d}{\partial z^2} = 0, \quad (13)$$

and the boundary conditions can be represented as

$$\left.\frac{\partial u_p}{\partial z}\right|_{z=-g} + \frac{B_{p2}}{c_{44}} m_{px} m_{pz} = 0, \quad (14)$$

$$\left.\frac{\partial u_p}{\partial z}\right|_{z=-g+p} + \frac{B_{p2}}{c_{44}} m_{px} m_{pz} = \left.\frac{\partial u_d}{\partial z}\right|_{z=-g+p} + \frac{B_{d2}}{c_{44}} m_{dx} m_{dz}, \quad (15)$$

$$u_p\big|_{z=-g+p} = u_d\big|_{z=-g+p}, \quad (16)$$

$$\left.\frac{\partial u_d}{\partial z}\right|_{z=g} + \frac{B_{d2}}{c_{44}} m_{dx} m_{dz} = 0. \quad (17)$$

This is a problem for elastic displacement functions u_p and u_d satisfying second-order wave equations with the zero right-hand sides (i.e., homogeneous equations). The problem is considered in combination with the boundary conditions for the same displacement functions containing, as parameters, time-dependent functions of the magnetization components (i.e., the boundary conditions that are inhomogeneous with respect to the displacements). In order to solve this problem, we follow [22] and separate it into a homogeneous part and an inhomogeneous part by analogy with the case of a single layer [20].

4. SEPARATION OF THE PROBLEM FOR THE ELASTICITY INTO TWO PROBLEMS

Since complete problem (12)–(17) for the elasticity contains, as parameters, magnetizations, we separate this problem into two ones. In the first problem, only the boundary conditions depend on the magnetization; and, in the second problem, only the equations depend on the magnetization.

To this end, we represent u_p and u_d in the form

$$u_p(z,t) = U_p(z,t) + v_p(z,t), \quad (18)$$

$$u_d(z,t) = U_d(z,t) + v_d(z,t), \quad (19)$$

where U_p and U_d are assumed to solve the homogeneous equations and satisfy the boundary conditions depending on the magnetization and v_p and v_d are assumed to solve the inhomogeneous equations where the character of inhomogeneity is determined by functions U_p and U_d but the boundary conditions are independent of the magnetization.

Substituting (18) and (19) into (12)–(17), we separate complete problem (12)–(17) into two individual problems.

For *problem no. 1* for $U_p(z,t)$ and $U_d(z,t)$, the equations have the form

$$\frac{\partial^2 U_p}{\partial z^2} = 0, \quad (20)$$

$$\frac{\partial^2 U_d}{\partial z^2} = 0, \quad (21)$$

and the boundary conditions are as follows:

$$\left.\frac{\partial U_p}{\partial z}\right|_{z=-g} = -\frac{B_{p2}}{c_{44}} m_{px} m_{pz}, \quad (22)$$

$$\left.\frac{\partial U_p}{\partial z}\right|_{z=-g+p} + \frac{B_{p2}}{c_{44}} m_{px} m_{pz} = \left.\frac{\partial U_d}{\partial z}\right|_{z=-g+p} + \frac{B_{d2}}{c_{44}} m_{dx} m_{dz}, \quad (23)$$

$$U_p\big|_{z=-g+p} = U_d\big|_{z=-g+p}, \quad (24)$$

$$\left.\frac{\partial U_d}{\partial z}\right|_{z=g} = -\frac{B_{d2}}{c_{44}} m_{dx} m_{dz}. \quad (25)$$

For *problem no. 2* for $v_p(z,t)$ and $v_d(z,t)$. The equations have the form

$$\frac{\partial^2 v_p}{\partial t^2} + 2\delta \frac{\partial v_p}{\partial t} - \frac{c_{44}}{\rho} \frac{\partial^2 v_p}{\partial z^2} = -\frac{\partial^2 U_p}{\partial t^2} - 2\delta \frac{\partial U_p}{\partial t}, \quad (26)$$

$$\frac{\partial^2 v_d}{\partial t^2} + 2\delta \frac{\partial v_d}{\partial t} - \frac{c_{44}}{\rho} \frac{\partial^2 v_d}{\partial z^2} = -\frac{\partial^2 U_d}{\partial t^2} - 2\delta \frac{\partial U_d}{\partial t}, \quad (27)$$

and the boundary conditions are as follows:

$$\left.\frac{\partial v_p}{\partial z}\right|_{z=-g} = 0, \quad (28)$$

$$\left.\frac{\partial v_p}{\partial z}\right|_{z=-g+p} = \left.\frac{\partial v_d}{\partial z}\right|_{z=-g+p}, \quad (29)$$

$$v_p\big|_{z=-g+p} = v_d\big|_{z=-g+p}, \quad (30)$$

$$\left.\frac{\partial v_d}{\partial z}\right|_{z=g} = 0. \quad (31)$$

Problem no. 1 does not contain functions $v_{p,d}$ and, therefore, can be solved independently. Functions $U_{p,d}$ obtained as a result of the solution of this problem should be substituted into problem no. 2. The complete solution to the entire problem is determined by formulas (18) and (19). First, let us consider problem no. 1 for $U_p(z,t)$ and $U_d(z,t)$. Integrating twice Eqs. (20) and (21) and substituting the obtained solutions into boundary conditions (22)–(25), we arrive at a system of four equations for the determination of four integration constants. Only three equations in this system are independent. Assuming that the z-independent component of function U_p is zero, we obtain a solution to problem (20)–(25) in the form

$$U_p = -\frac{B_{p2}}{c_{44}} m_{px} m_{pz} z, \quad (32)$$

$$U_d = -\frac{B_{d2}}{c_{44}} m_{dx} m_{dz} z - \frac{-g+p}{c_{44}} \times \left(B_{p2} m_{px} m_{pz} - B_{d2} m_{dx} m_{dz}\right). \quad (33)$$

As is seen, both of these expressions linearly depend on coordinate z and they coincide when $z = -g + p$.

Let us introduce the notation

$$\alpha = -\frac{B_{p2}}{2c_{44}} m_{px} m_{pz}, \tag{34}$$

$$\beta = -\frac{B_{d2}}{2c_{44}} m_{dx} m_{dz}, \tag{35}$$

$$\gamma = \frac{(g-p)}{2c_{44}} \left(B_{p2} m_{px} m_{pz} - B_{d2} m_{dx} m_{dz} \right). \tag{36}$$

Then, we obtain

$$U_p = \begin{cases} 2\alpha z \text{ when } -g \le z \le -g + p, \\ 0 \text{ when } -g + p \le z \le g, \end{cases} \tag{37}$$

$$U_d = \begin{cases} 0 \text{ when } -g \le z \le -g + p, \\ 2(\beta z + \gamma) \text{ when } -g + p \le z \le g. \end{cases} \tag{38}$$

Thus, problem no. 1 is solved, and we can pass to problem no. 2 (26)–(31). However, since this problem is inhomogeneous (having the nonzero right-hand side of Eqs. (26) and (27)), its solution can be represented only in the form of a series of the eigenfunctions of the coordinate part of the corresponding homogeneous problem with the zero boundary conditions for the entire structure [22]. Accordingly, functions U_p and U_d entering the right-hand sides of Eqs. (26) and (27) also should be decomposed in a series of the same eigenfunctions.

5. THE EIGENFUNCTIONS OF THE COORDINATE PART OF THE HOMOGENEOUS PROBLEM FOR THE ENTIRE STRUCTURE

Consider the coordinate part of the homogeneous problem for the entire structure. According to the general geometry of the problem (see Fig. 1), the origin is at the center of the structure and its total length is $2g$, i.e., the beginning and end of the structure have equal absolute values of coordinates: $z_1 = -g$ and $z_2 = g$.

We have the following even and odd eigenfunctions:

$$y_n = \frac{1}{\sqrt{g}} \cos\left(\frac{\pi n}{g} x \right) \tag{39}$$

and

$$y_n = \frac{1}{\sqrt{g}} \sin\left[\frac{\pi}{g} \left(n + \frac{1}{2} \right) x \right], \tag{40}$$

respectively, where n is an arbitrary integer.

6. DECOMPOSITION OF FUNCTION $U_{p,d}(z)$ IN A SERIES OF THE EIGENFUNCTIONS OF THE HOMOGENEOUS PROBLEM

Consider the decomposition of function $U_{p,d}(z)$ in a series of eigenfunctions (39), (40). Complete function $U(z)$ is represented by a broken curve consisting of two straight-line sections. According to the general technique of decomposition in a Fourier series [23], first, such a function should be represented as a sum of two partial functions. Each of these functions is represented by a straight-line section and equals zero on both sides of this section. Next, each partial function should be represented as a sum of an even part and an odd part. After that, each of these parts is separately decomposed in series of even and odd eigenfunctions. Original function $U(z)$ is the sum of all of these series. Following this procedure, we obtain the decomposition of function U_p in the form

$$U_p = U_{pv0} + \sum_{n=1}^{\infty} U_{pvn} \cos\left(\frac{\pi n}{g} z \right) + \sum_{n=1}^{\infty} U_{pwn} \sin\left[\frac{\pi (2n-1)}{2g} z \right], \tag{41}$$

where

$$U_{pv0} = \alpha V_{pv0}, \tag{42}$$

$$U_{pvn} = \alpha V_{pvn}, \tag{43}$$

$$U_{pwn} = \alpha V_{pwn}, \tag{44}$$

with

$$V_{pv0} = -\frac{p(2g-p)}{2g}, \tag{45}$$

$$V_{pvn} = \frac{2g}{\pi^2} \frac{1}{n^2} \left\{ (-1)^{n-1} + \cos\left[\frac{\pi (g-p)}{g} n \right] + \left[\frac{\pi (g-p)}{g} n \right] \sin\left[\frac{\pi (g-p)}{g} n \right] \right\}, \tag{46}$$

$$V_{pwn} = \frac{8g}{\pi^2} \frac{1}{(2n-1)^2} \left\{ (-1)^{n-1} - \sin\left[\frac{\pi (g-p)}{2g} (2n-1) \right] + \left[\frac{\pi (g-p)}{2g} (2n-1) \right] \cos\left[\frac{\pi (g-p)}{2g} (2n-1) \right] \right\}. \tag{47}$$

In a similar manner, we decompose function U_d:

$$U_d = U_{dv0} + \sum_{n=1}^{\infty} U_{dvn} \cos\left(\frac{\pi n}{g} z \right) + \sum_{n=1}^{\infty} U_{dwn} \sin\left[\frac{\pi (2n-1)}{2g} z \right], \tag{48}$$

where

$$U_{dv0} = \beta V_{dv0} + \gamma W_{dv0}, \tag{49}$$

$$U_{dvn} = \beta V_{dvn} + \gamma W_{dvn}, \tag{50}$$

$$U_{dwn} = \beta V_{dwn} + \gamma W_{dwn} \tag{51}$$

with

$$V_{dv0} = \frac{p(2g-p)}{2g}, \tag{52}$$

$$W_{dv0} = \frac{(2g-p)}{g}, \tag{53}$$

$$V_{dvn} = \frac{2g}{\pi^2}\frac{1}{n^2}\left\{(-1)^n - \cos\left[\frac{\pi(g-p)}{g}n\right] - \left[\frac{\pi(g-p)}{g}n\right]\sin\left[\frac{\pi(g-p)}{g}n\right]\right\}, \tag{54}$$

$$W_{dvn} = \frac{2}{\pi}\left(\frac{1}{n}\right)\sin\left[\frac{\pi(g-p)}{g}n\right], \tag{55}$$

$$V_{dwn} = \frac{8g}{\pi^2}\frac{1}{(2n-1)^2}\left\{(-1)^{n-1} + \sin\left[\frac{\pi(g-p)}{2g}(2n-1)\right] - \left[\frac{\pi(g-p)}{2g}(2n-1)\right]\cos\left[\frac{\pi(g-p)}{2g}(2n-1)\right]\right\}, \tag{56}$$

$$W_{dwn} = \frac{4}{\pi}\frac{1}{(2n-1)}\cos\left[\frac{\pi(g-p)}{2g}(2n-1)\right]. \tag{57}$$

Now, consider problem no. 2 for $v_p(z,t)$ and $v_d(z,t)$ of form (26)–(31). We seek for a solution to the problem in the form of a decomposition in the eigenfunctions of homogeneous problem (39), (40) for layer p:

$$v_p = v_{pv0} + \sum_{n=1}^{\infty} v_{pvn}\cos\left(\frac{\pi n}{g}z\right) + \sum_{n=1}^{\infty} v_{pwn}\sin\left[\frac{\pi(2n-1)}{2g}z\right], \tag{58}$$

where functions v_{pv0}, v_{pvn}, and v_{pwn} depend on time only and are to be determined. Replacing index p by d, we obtain a similar solution for layer d. The solutions represented in this form automatically satisfy boundary conditions (28)–(31).

The substitution of functions v_p and U_p into (26) yields an equation whose left-hand side contains a free term, the z-depending sines and cosines involved in the eigenfunctions, and the zero right-hand side. This equation can be satisfied only when the free terms and the coefficients of the sines and cosines are zero. A similar equation is obtained from (27) for layer d.

As result, we arrive at the equations for the decomposition coefficients of functions v_p and v_d for layers p and d.

We have the equations

$$\frac{\partial^2 v_{pv0}}{\partial t^2} + 2\delta\frac{\partial v_{pv0}}{\partial t} = -V_{pv0}\left(\frac{\partial^2\alpha}{\partial t^2} + 2\delta\frac{\partial\alpha}{\partial t}\right), \tag{59}$$

$$\frac{\partial^2 v_{pvn}}{\partial t^2} + 2\delta\frac{\partial v_{pvn}}{\partial t} + \frac{c_{44}}{\rho}\left(\frac{\pi n}{g}\right)^2 v_{pvn} = -V_{pvn}\left(\frac{\partial^2\alpha}{\partial t^2} + 2\delta\frac{\partial\alpha}{\partial t}\right), \tag{60}$$

$$\frac{\partial^2 v_{pwn}}{\partial t^2} + 2\delta\frac{\partial v_{pwn}}{\partial t} + \frac{c_{44}}{\rho}\left[\frac{\pi(2n-1)}{2g}\right]^2 v_{pwn} = -V_{pwn}\left(\frac{\partial^2\alpha}{\partial t^2} + 2\delta\frac{\partial\alpha}{\partial t}\right) \tag{61}$$

for layer p and

$$\frac{\partial^2 v_{dv0}}{\partial t^2} + 2\delta\frac{\partial v_{dv0}}{\partial t} = -V_{dv0}\left(\frac{\partial^2\beta}{\partial t^2} + 2\delta\frac{\partial\beta}{\partial t}\right) - W_{dv0}\left(\frac{\partial^2\gamma}{\partial t^2} + 2\delta\frac{\partial\gamma}{\partial t}\right), \tag{62}$$

$$\frac{\partial^2 v_{dvn}}{\partial t^2} + 2\delta\frac{\partial v_{dvn}}{\partial t} + \frac{c_{44}}{\rho}\left(\frac{\pi n}{g}\right)^2 v_{dvn} = -V_{dvn}\left(\frac{\partial^2\beta}{\partial t^2} + 2\delta\frac{\partial\beta}{\partial t}\right) - W_{dvn}\left(\frac{\partial^2\gamma}{\partial t^2} + 2\delta\frac{\partial\gamma}{\partial t}\right), \tag{63}$$

$$\frac{\partial^2 v_{dwn}}{\partial t^2} + 2\delta\frac{\partial v_{dwn}}{\partial t} + \frac{c_{44}}{\rho}\left[\frac{\pi(2n-1)}{2g}\right]^2 v_{dwn} = -V_{dwn}\left(\frac{\partial^2\beta}{\partial t^2} + 2\delta\frac{\partial\beta}{\partial t}\right) - W_{dwn}\left(\frac{\partial^2\gamma}{\partial t^2} + 2\delta\frac{\partial\gamma}{\partial t}\right) \tag{64}$$

for layer d.

Thus, problem no. 2 is solved. The complete system of equations for the original problem includes the equations for magnetization vector components $m_{p,dx,y,z}$ of form (2) in combination with equations (59)–(64) for functions $v_{p,dx,y}$. However, the obtained system does not enable us to find in a pure form the sought time dependences of magnetizations and displacements, because effective fields (3)–(6), entering the equations for magnetizations, and time derivatives of functions α, β, and γ (34)–(36), containing the same fields, involve at this stage coordinate derivatives $\partial u_{p,dx,y}/\partial z$ of displacements and these derivatives are not yet determined. In order to remove the indeterminacy, we follow study [20] and use the z-averaged values of these derivatives.

We retain their time dependences using the derivatives in the form

$$\frac{\partial u_p}{\partial z} = 2\alpha - \sum_{n=1}^{\infty} v_{pvn} S_{psn} + \sum_{n=1}^{\infty} v_{pwn} C_{psn}, \quad (65)$$

$$\frac{\partial u_d}{\partial z} = 2\beta - \sum_{n=1}^{\infty} v_{dvn} S_{dsn} + \sum_{n=1}^{\infty} v_{dwn} C_{dsn}, \quad (66)$$

where

$$S_{psn} = \frac{1}{p}\left\{(-1)^n - \cos\left[\frac{\pi(g-p)}{g}n\right]\right\}, \quad (67)$$

$$C_{psn} = \frac{1}{p}\left\{(-1)^{n-1} - \sin\left[\frac{\pi(g-p)}{2g}(2n-1)\right]\right\}, \quad (68)$$

$$S_{dsn} = \frac{1}{(2g-p)}\left\{(-1)^{n-1} + \cos\left[\frac{\pi(g-p)}{g}n\right]\right\}, \quad (69)$$

$$C_{dsn} = \frac{1}{(2g-p)}\left\{(-1)^{n-1} + \sin\left[\frac{\pi(g-p)}{2g}(2n-1)\right]\right\}. \quad (70)$$

7. THE FORM OF THE SOLUTION TO THE COMPLETE PROBLEM FOR THE ELASTICITY

Thus, solution to the complete problem for the elasticity (18)–(19) takes the form

$$u_p = 2\alpha z + v_{pv0} + \sum_{n=1}^{\infty} v_{pvn}\cos\left(\frac{\pi n}{g}z\right) + \sum_{n=1}^{\infty} v_{pwn}\sin\left[\frac{\pi(2n-1)}{2g}z\right], \quad (71)$$

$$u_d = 2(\beta z + \gamma) + v_{dv0} + \sum_{n=1}^{\infty} v_{dvn}\cos\left(\frac{\pi n}{g}z\right) + \sum_{n=1}^{\infty} v_{dwn}\sin\left[\frac{\pi(2n-1)}{2g}z\right]. \quad (72)$$

The above expressions are obtained for the x component of the elastic displacement. For the y component, the components corresponding to the y coordinate should be used in these expressions.

8. REDUCTION OF THE COMPLETE PROBLEM TO A FORM SUITABLE FOR NUMERICAL SOLUTION

Thus, the complete system of equations for time-dependent magnetizations and displacements contains six first-order equations for magnetization components $m_{p,dx,y,z}$ of form (2) and $4 + 8n$ second-order equations of form (59)–(64) for displacement functions $v_{p,dx,y}$. We apply the standard procedure of reducing one second-order equation to two first-order equations [23] to obtain from the latter $8 + 16n$ first-order equations. Thus, the complete system of first-order equations for the magnetizations and elastic displacements that is suitable for numerical solution contains $6 + 8 + 16n = 14 + 16n$ equations, where n is the number of terms in the decomposition in the eigenfunctions of the homogeneous problem.

A test calculation shows that, in the presence of one term ($n = 1$), the accuracy of the decomposition is about 15–20% and five terms ($n = 5$) ensure an accuracy no worse than 5%.

When the series is truncated to one term ($n = 1$), we obtain six first-order equations for the magnetizations and 24 first-order equations for the elastic displacement components, i.e., 30 first-order equations total. In the study, this system of equations is solved with the help of the fourth-order Runge–Kutta method [23]. As a result, the time evolution of magnetization oscillations and displacement vibrations excited by an alternate field is obtained.

9. ESTIMATION OF THE ACCURACY OF THE OBTAINED RESULTS AND POSSIBILITY OF ITS ENHANCEMENT

System of equations (2), (59)–(64) has been derived within a number of approximations applied to simplify the problem. These approximations to a certain degree affect the accuracy of the calculation results. Thus, the magnetic oscillations in both layers are assumed to be uniform, the elastic displacements perpendicular to the structure plane are not considered, and the derivative of the displacement with respect to the z coordinate is disregarded. In addition, the numerical computation is performed within the approximation of the first-mode elastic vibrations; i.e., all of the subsequent decomposition terms are disregarded.

It is important to assess to what extent the assumed approximations provide for the sufficient accuracy of the calculation.

To this end, we consider some limit cases. Thus, a test has shown that, relative to the splitting of the structure into layers, the solution is completely specularly symmetric; i.e., when layer thicknesses p and d are interchanged and, simultaneously, magnetizations m_p and m_d are interchanged, the layer magnetization oscillations are retained and the sum of elastic displacement vibrations on the opposite surfaces of the structure reverses the sign; i.e., in this context, the situation is absolutely correct.

For the case when the magnetizations of both layers are equal, we consider the amplitudes of magnetic oscillations and elastic vibrations as functions of the relative change of the layers' thicknesses, the thickness of the entire structure being retained. Obviously, the oscillation and vibration amplitudes should not

change in this case, because the situation completely coincides with the case of a single-layer magnetic plate [20]. However, a certain small change has been revealed for problem parameters similar to the aforementioned ones.

Thus, when layer thickness p changes from 0.1 to 0.9 (0.2 to 0.8) and, correspondingly, d changes from 0.9 to 0.1 (0.8 to 0.2) of the total thickness of the structure, the change of magnetic oscillation amplitudes reaches 16% (decreases to 12%). The change of elastic vibration amplitudes is 19% and 16%, respectively, under the same conditions.

Thus, we can believe that the accuracy of magnetic oscillation and elastic vibration amplitudes obtained in this study is no worse than 12–19%, a value that quite satisfactory for most applications (for example, for excitation of hypersound in an exterior medium).

The simplest way to additionally enhance the calculation accuracy is to take into account next series terms. However, the most radical decision is to consider the magnetization that is nonuniform across the thickness of each layer; then, it will also be unnecessary to average the derivative of the displacement over the thickness. Taking into account elastic displacements perpendicular to the structure plane, we not only enhance the accuracy but also can reveal the possibility of excitation of new elastic vibration modes having a 3D character, a circumstance that can improve the functional potentialities of technical devices.

10. TIME EVOLUTION OF OSCILLATIONS

Consider the results of numerical computation of the time evolution of oscillations for various frequencies of magnetic resonances of individual layers. These results are partly obtained in [21].

Time dependences of magnetization and displacement components $m_{p,dx}$ and $u_{p,dx}$, respectively, on the exterior surfaces of the structure are depicted in Fig. 2 for the linear and nonlinear modes.

For the parameters of the material and structure geometry indicated in the figure caption, the frequency of the elastic resonance for the first mode of the entire structure and the frequency of the linear magnetic resonance in layer p are equal to the excitation frequency 2800 MHz, while the frequency of the linear magnetic resonance in layer d is lower: 2380 MHz. For the assumed attenuation parameters, the times of formation of the stationary amplitudes of both kinds of oscillations approach the value 2×10^{-9} s.

It is seen from Figs. 2a and 2b that, in the linear mode, both kinds of oscillations in layer p gradually increase without beating; while, in layer d, oscillations increase with slight beating. After stationary oscillations are formed, the amplitudes of both kinds of oscillations in layer d are approximately half as high as those in layer p. The advance of the magnetic oscillation phase in layer d over the phase in layer p is about 90°, and the lag of the elastic vibration phase in layer d behind the phase in layer p has the same value.

It is seen from Figs. 2c and 2d that magnetic oscillations in both layers evolve with beating, while elastic vibrations evolve without beating. After stationary oscillations are formed, the amplitudes of both kinds of oscillations in layer d exceed those in layer p: the amplitude of magnetic oscillations is higher by a factor of 1.2 and the amplitude of elastic vibrations is higher by a factor of 1.5. The phases of magnetic oscillations in both layers coincide, and the phases of elastic vibrations in layers p and d differ by 180°; i.e., the opposite surfaces of the structure move in antiphase.

The comparison of the modes show that

(i) the amplitude of magnetic oscillations in the nonlinear mode exceeds the amplitude of these oscillations in the linear mode by a factor of 38 in layer p and 110 in layer d,

(ii) the amplitude of elastic vibrations in the nonlinear mode exceeds the amplitude of these oscillations in the linear mode by a factor of 33 in layer p and 71 in layer d.

These peculiarities are due to the fact that the linear-mode magnetic resonance characteristics in both layers have a narrow symmetric bell-shaped form and do not overlap. The resonance frequency in layer p equals the excitation frequency, and the stationary amplitude takes the maximum value possible for the attenuation parameter. However, for layer d, the excitation frequency is higher than the resonance frequency, a circumstance that causes beating and do not allow the amplitude to evolve to the maximum. The elastic vibration amplitudes in both layers are proportional to the magnetic oscillation amplitude, and, therefore, the elastic vibration amplitude is lower in layer d than in layer p.

In the nonlinear mode, the magnetic resonance curves in both layers substantially spread, are nonsymmetric, and have the form of wide triangles with vertices deflected toward high frequencies, which is due to the traditional detuning mechanism [24, 25]. When the excitation amplitude is high enough, the inclined vertex of the resonance curve of layer d reaches the excitation frequency. As a result, the magnetic oscillation amplitude in this layer abruptly increases leading to the growth of the elastic vibration amplitude, a circumstance that accounts for the excess of the both kinds of oscillations amplitudes in this layer over the same oscillations in layer p.

The relative phase shift of linear magnetic oscillations in layers p and d is caused by the difference of their resonance frequencies and corresponds to the known phase shift of forced oscillations beyond the resonance conditions [24]. The phase shift of elastic vibrations is a result of the superposition of magnetic oscillations in different layers and is observed when it

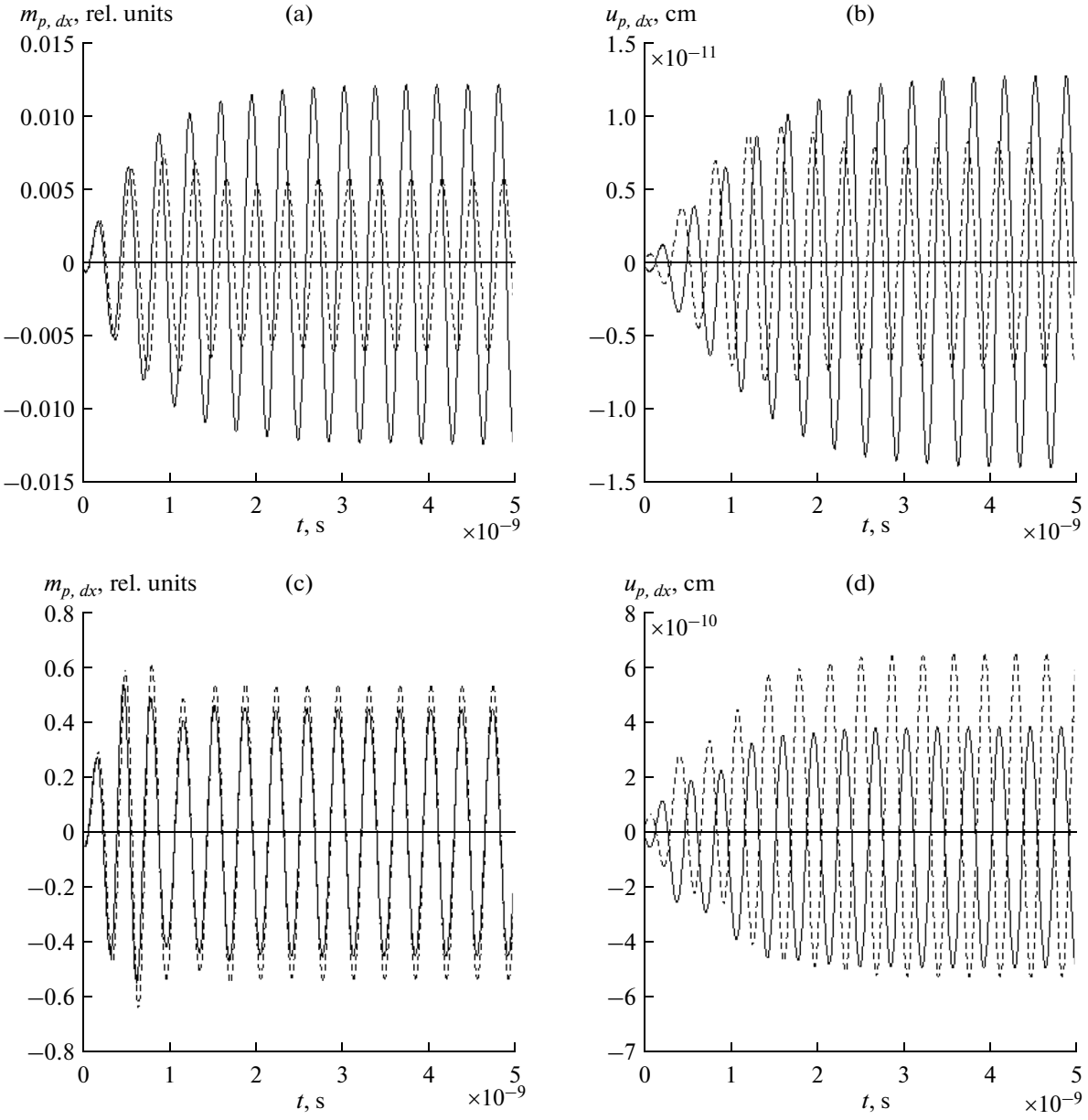

Fig. 2. Magnetization oscillations $m_{p,dx}$ and displacement vibrations $u_{p,dx}$ vs. time for layers (solid lines) p and (dashed lines) d in the (a, b) linear and (c, d) nonlinear modes. The material parameters are as follows: $4\pi M_{p0} = 1750$ G, $4\pi M_{d0} = 1900$ G, $B_{p2} = B_{d2} = 13.92\times10^6$ Erg cm^{-3}, $c_{44} = 7.64\times10^{11}$ Erg cm^{-3}, $K_{p1} = K_{d1} = 0$, $\alpha_p = \alpha_d = 0.04$, $\delta = 2\times10^9$ s^{-1}. The parameters of the structure's geometry are as follows: $2g = 0.6865$ μm, $p = 0.3\times2g = 0.206$ μm, and $d = 0.7\times2g = 0.481$ μm. The excitation parameters are as follows: $F = 2800$ MHz, $H_0 = 2750$ Oe, $h_0 =$ (a, b) 1 and (c, d) 100 Oe, and the polarization of the alternate field is circular such that $h_x = h_0\sin(2\pi Ft)$ and $h_y = -h_0\cos(2\pi Ft)$.

is taken into account that the structure is an entire elastic vibrating system.

In the nonlinear mode, all of the three systems—elastic and both magnetic ones—are excited under the resonance conditions. Therefore, the magnetic oscillation phases in both layers coincide and the elastic vibration phases on the opposite surfaces of the structure are opposite, which resembles the character of the first mode of vibrations of the ends of a string with free ends [22].

Note a certain nonsymmetry in displacement vibrations that is observed in Fig. 2d: the time sweep of vibrations is shifted with respect to the center axis downward in the figure by 10^{-10} cm for layer p, and upward by approximately the same value for layer d. This nonsymmetry means that, in the nonlinear

mode, the time-average thickness of the entire structure increases by approximately 3×10^{-6} of its initial value.

The nonsymmetry can apparently be attributed to the nonsymmetry of the boundary conditions imposed on different surfaces of each layer: the interior surfaces of the layers contact, while the exterior ones are free. The additional nonequivalence of the boundary conditions for both layers is due to the difference of the magnetizations, which is especially pronounced in the nonlinear mode.

11. EXPERIMENTAL CONDITIONS OF OBSERVATION OF THE DESCRIBED PHENOMENA

The presented solution to the considered problem enables us to determine the normalized oscillation amplitudes for magnetizations m_p and m_d in each layer and the vibration amplitudes for elastic displacements u_p and u_d when the values of coordinate z in each individual layer are specified. However, in real experiments, it is of interest to control the total magnetization of the entire structure regarded as a single sample as well as the elastic displacements of the exterior surfaces of the structure relative to each other. Therefore, it is important to find the coupling between really measured amplitudes of total magnetization m_S and elastic displacement u_S on the one hand and amplitudes $m_{p,d}$ and $u_{p,d}$ obtained above on the other hand.

The investigation of the time evolution of oscillations shows that, when the magnetic and elastic resonance frequencies are different, there are rather intricate phase relationships between excited oscillations. These relationships should be taken into account in the calculation of the total amplitudes.

Thus, the total magnetization of the entire structure is determined by the sum of the relative contributions of the magnetizations of each layer with allowance for the phase difference:

$$m_S \cos(\omega t + \varphi_S) = m_p \frac{p}{p+d} \cos(\omega t + \varphi_p) + m_d \frac{d}{p+d} \cos(\omega t + \varphi_d), \quad (73)$$

where φ_p and φ_d are phase shifts of excited magnetization oscillations in layers p and d relative to the alternate field phase and m_S and φ_S are the amplitude and phase, respectively, of the resulting oscillations in the entire structure.

When a double-layer structure is used for hypersound excitation in the exterior medium, one of the surfaces should be rigidly fixed on a massive support, while the other surface remains free and is an exciter of such a kind. In this case, the vibrations of the unfixed surface are determined by the trigonometric sum of the oscillations on the opposite surfaces of the structure:

$$u_S \cos(\omega t + \varphi_S) = u_p \cos(\omega t + \varphi_p) + u_d \cos(\omega t + \varphi_d). \quad (74)$$

As is seen from formulas (73) and (74), the amplitude of excited vibrations depends on the phase relationships between the vibrations of individual layers. In certain special cases, the phase relationships are rather simple despite their intricate general character.

Case no. 1. The elastic resonance frequency and the frequencies of both magnetic resonances are equal to the excitation frequency. Then, the magnetic oscillations in both layers are in phase, and the elastic vibrations on the opposite surfaces of the structure are in antiphase. This case is similar to the case of a single magnetic plate considered in [20].

Case no. 2. The elastic resonance frequency is equal to the excitation frequency, one of the magnetic resonance frequencies is higher and the other one is lower than the excitation frequency by equal values. In the linear mode, the phase relationships are rather intricate; however, in a strongly nonlinear mode, the magnetic oscillations (elastic vibrations) of individual layers approach the in-phase (antiphase) state; i.e., despite the difference of the layer magnetizations, the phase relationships between oscillations become similar to those in the previous case.

Owing to the in-phase magnetic oscillations of the layers, the amplitude of the total magnetic oscillations in both of these cases takes the form

$$m_S = m_p \frac{p}{p+d} + m_d \frac{d}{p+d}. \quad (75)$$

Similarly, owing to the antiphase elastic vibrations observed when one of the structure surfaces is fixed, the amplitude of elastic vibrations on the free surface has the form

$$u_S = u_p - u_d, \quad (76)$$

or

$$u_S = |u_p| + |u_d|. \quad (77)$$

The time dependence of oscillations for case no. 1 (2) is depicted in Figs. 3a and 3b (Figs. 3c and 3d). The following conclusions can be drawn from Fig. 3. The curves for m_p and m_d in Fig. 3a coincide because both layers have identical parameters; in this situation, total amplitude m_S doubles. The curves for u_p and u_d in Fig. 3b have identical amplitudes, are in antiphase, and, as a result, total amplitude u_S also doubles. The curves for m_p and m_d in Fig. 3c remain in phase but have different amplitudes, a circumstance that is due to the different magnetizations of the layers; amplitude m_S is also the sum of amplitudes m_p and m_d. The curves for u_p and u_d in Fig. 3d are also in antiphase but have different amplitudes following the magnetization

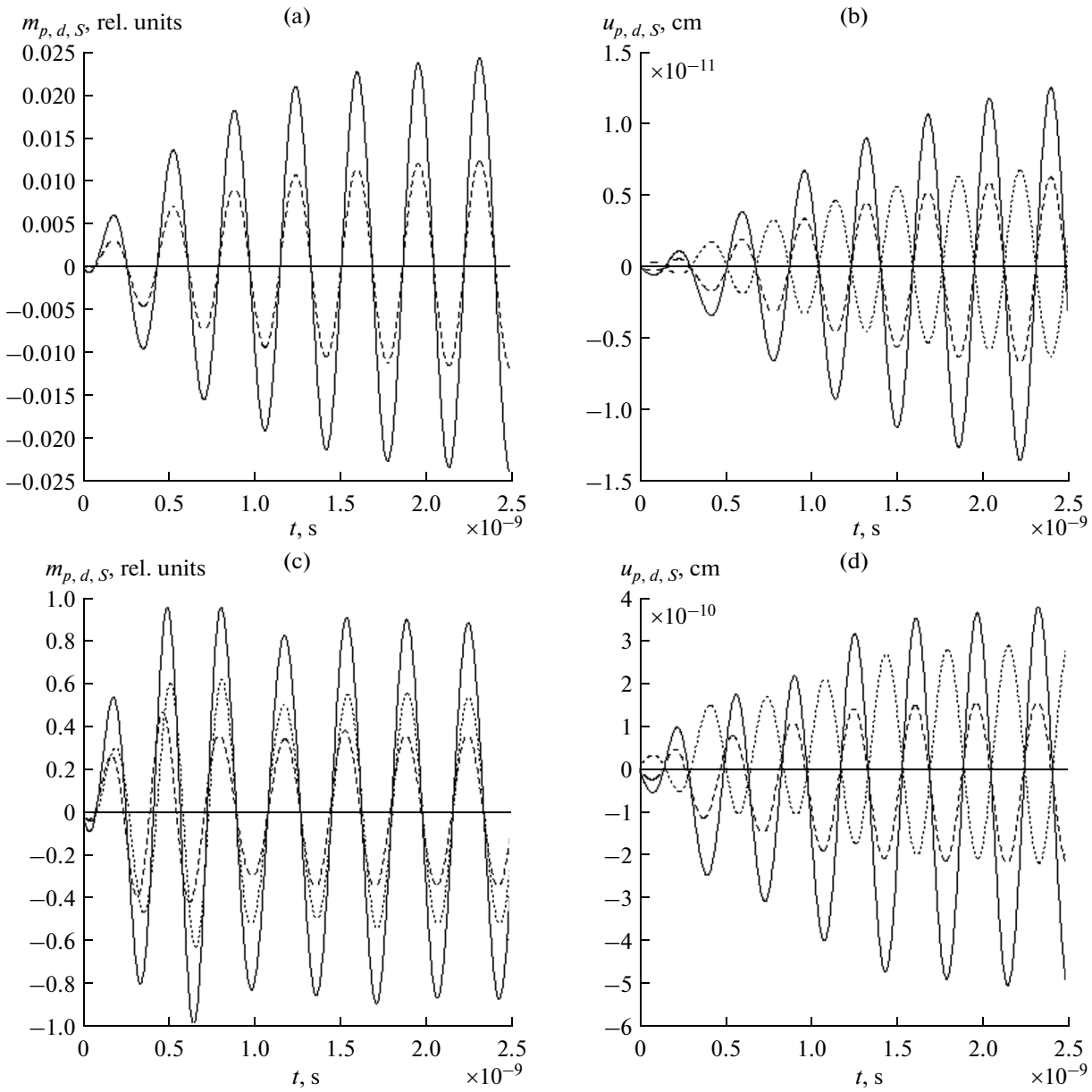

Fig. 3. (a, c) Magnetization oscillations $m_{p,d,S}$ and (b, d) displacement vibrations $u_{p,d,S}$ vs. time for layers (dashed lines) p and (dotted lines) d and for (solid lines) entire structure S. The parameters are as follows: (a, b) $4\pi M_{p0} = 1750$ G, $4\pi M_{d0} = 1750$ G, and $h_0 = 1$ Oe; (c, d) $4\pi M_{p0} = 1600$ G, $4\pi M_{d0} = 1900$ G, and $h_0 = 100$ Oe; the layers' thicknesses are $p = d = 0.5 \times 2g = 0.3432$ μm; and the remaining parameters are indicated in the caption of Fig. 2.

amplitudes of the corresponding layers. Oscillations u_S are also the algebraic sum of u_p and u_d, exhibit the shift of the zero value by -0.68×10^{-10} cm relative to the equilibrium position. This shift is similar to that from Fig. 2d and is attributed to the nonsymmetrical boundary conditions on different surfaces of each layer.

12. AMPLITUDE–FREQUENCY CHARACTERISICS

In practice, it is important to analyze the amplitude of oscillations excited within a certain frequency interval, primarily, near the magnetic and elastic resonances. In order to avoid the difficulties related with taking into account complicated phase relationship, we restrict the consideration to the two aforementioned cases: the first case, when the resonance frequencies of all oscillations coincide, and the second case, when one of the magnetic resonance frequencies is higher and the other one is lower than the elastic resonance frequency by equal values. Then, the first case is equivalent to the case of a single-layer structure considered in [20] and the second case characterizes the specificity of the double-layer character of the structure.

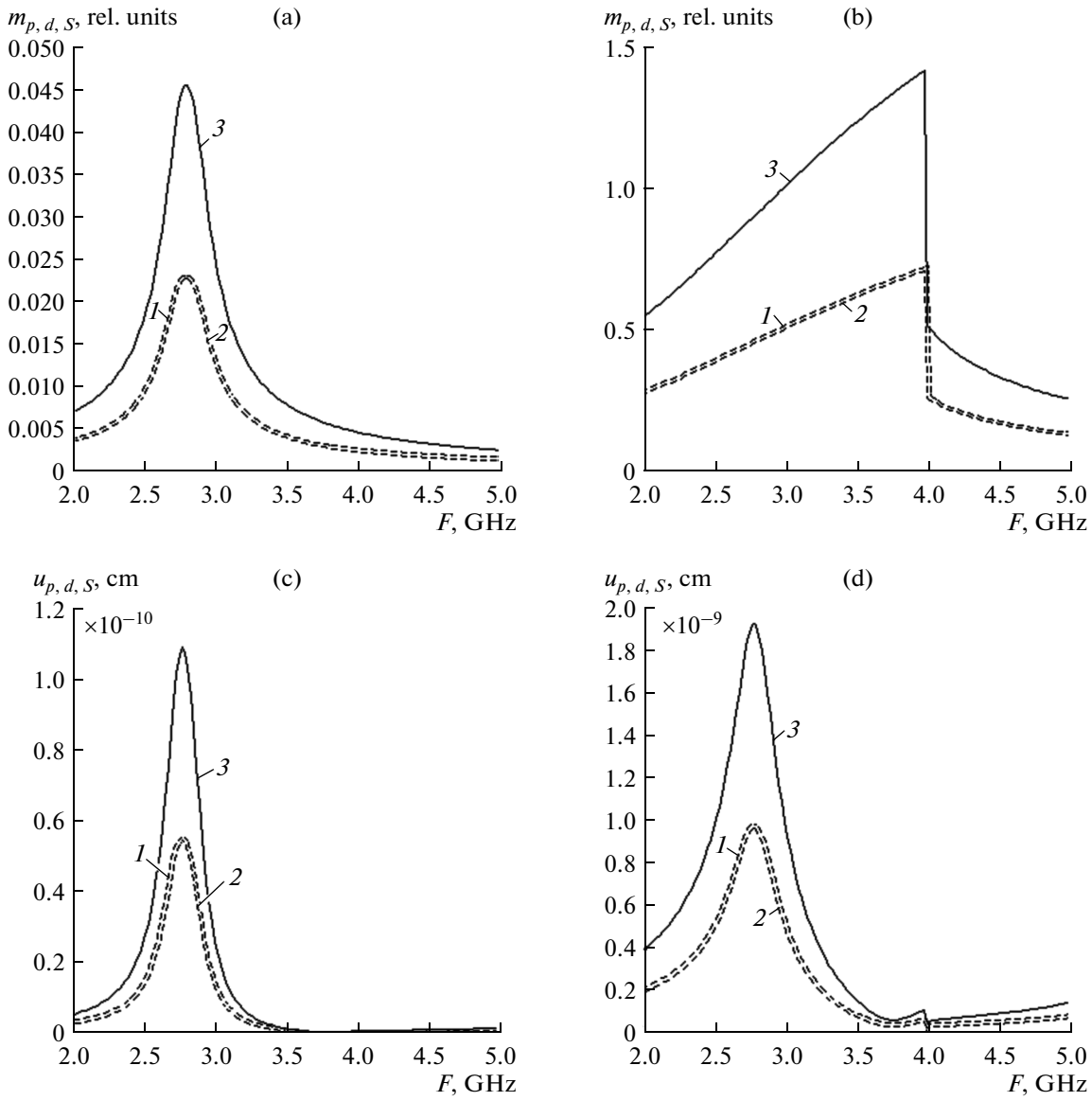

Fig. 4. Amplitude–frequency characteristics of the excitation of magnetic ($m_{p,d,S}$) oscillations and elastic ($u_{p,d,S}$) vibrations for the case when the frequencies of all resonances coincide in the (a, c) linear and (b, d) nonlinear modes: (*1*) layer p, (*2*) layer d, and (*3*) the total amplitude for the entire structure. The amplitude of the alternate field is $h_0 =$ (a, c) 1 and (b, d) 100 Oe and the polarization is circular. The parameters are as follows: $4\pi M_{p0} = 4\pi M_{d0} = 1750$ G, $p = d = 0.5 \times 2g = 0.3432$ μm, $H_0 = 2750$ Oe, and the remaining parameters are indicated in the caption of Fig. 2.

The amplitude–frequency characteristics (AFCs) of the linear- and nonlinear-mode excitations of magnetic oscillations and elastic vibrations are displayed in Figs. 4 and 5.The layer thicknesses are assumed equal, i.e., $p = d$. Curves *1* and *2* correspond to the oscillations for each individual layer, and curves *3* correspond to the total oscillations. Curves *3* for magnetic resonances are plotted as the sums of amplitudes $m_p + m_d$, i.e., the values in these curves are twice the value of m_S corresponding to formula (75). Curves *3* for elastic resonances are plotted as the sums $u_p + u_d$, corresponding to formula (77) taking into account that the processes are in antiphase.

For the first case, when the frequencies of all of the three resonances are identical and equal to 2.8 GHz, the corresponding characteristics are shown in Fig. 4. It is seen from the figure that the amplitudes of magnetic oscillations and elastic vibrations in individual layers (*1* and *2*) coincide, a circumstance that is due to the coincidence of the layers' parameters. The double dashed line for curves *1* and *2* is plotted for visualization, both curves coincide).

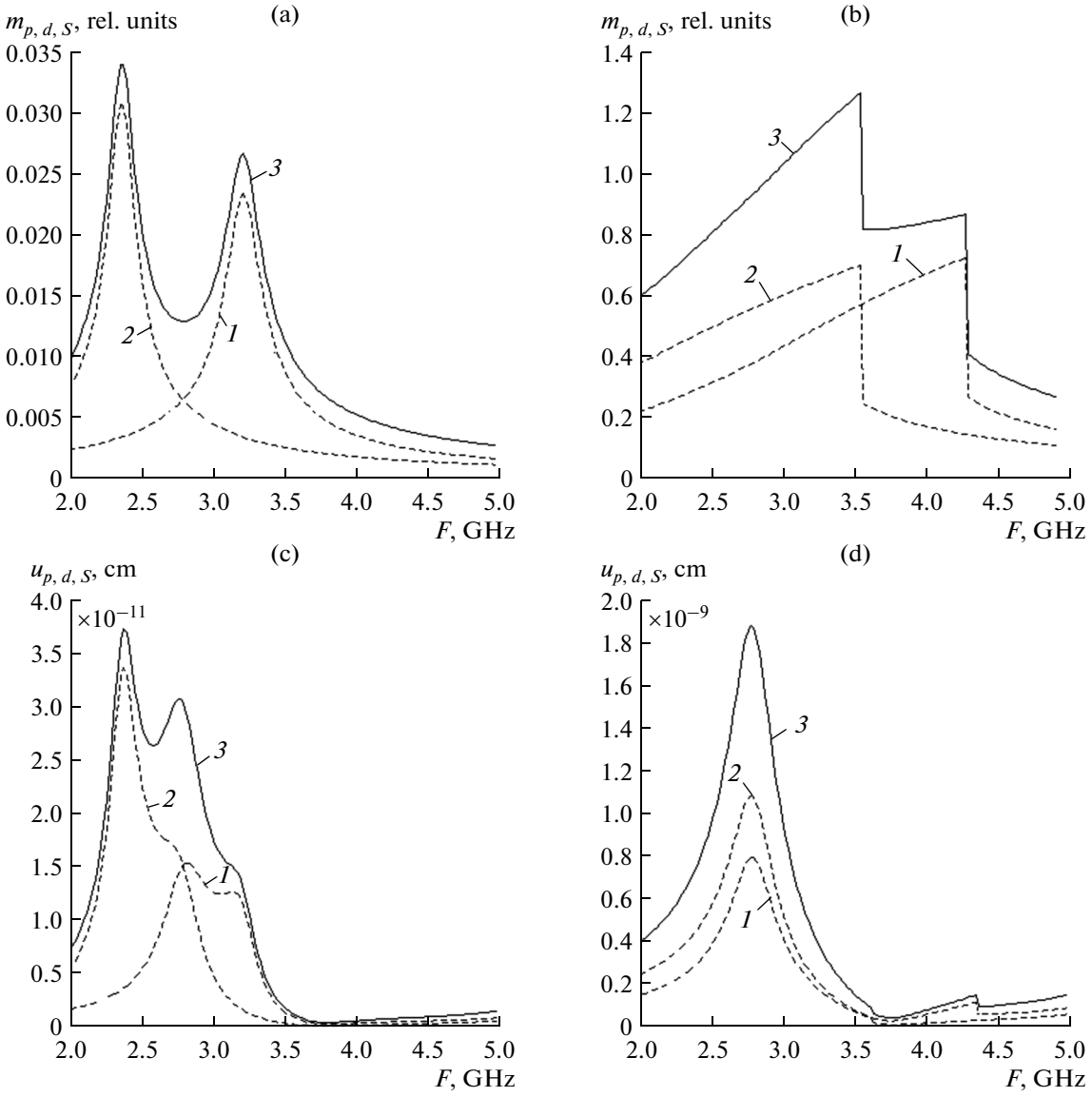

Fig. 5. Amplitude–frequency characteristics of the excitation of magnetic ($m_{p,d,S}$) oscillations and elastic ($u_{p,d,S}$) vibrations for the case of different resonance frequencies in the (a, c) linear and (b, d) nonlinear modes: (*1*) layer *p*, (*2*) layer *d*, and (*3*) the total amplitude for the entire structure. The amplitude of the alternate field is h_0 = (a, c) 1 and (b, d) 100 Oe and the polarization is circular. The parameters are as follows: $4\pi M_{p0} = 1600$ G, $4\pi M_{d0} = 1900$ G, $p = d = 0.5 \times 2g = 0.3432$ μm, $H_0 = 2750$ Oe, and the remaining parameters are indicated in the caption of Fig. 2.

In the linear mode, we have symmetric bell-shaped AFCs of magnetic oscillations (see Fig. 4a); while, in the nonlinear mode (see Fig. 4b), the vertices of the resonance curves are substantially deflected toward high frequencies, and, as a result, the AFCs acquire a triangular shape. This shape of the resonance curve corresponds to the amplitude limited because of the detuning mechanism [24, 25].

In the nonlinear mode, the amplitude increases at the linear resonance frequency 2.8 GHz by a factor of 18.5. Then, the AFC maximum moves to a frequency of 4 GHz and exceeds the linear-mode maximum by a factor of 30.9.

For elastic vibrations, the AFC in both modes (Figs. 4c, 4d) retains its more or less symmetric bell-shaped form. In the nonlinear mode, the steepness of its high-frequency slope exceeds the steepness of the low-frequency slope; however, this nonsymmetry is less pronounced than that for magnetic oscillations, because, here, there is no detuning mechanism limiting the amplitude.

The frequency of the resonance peak maximum is retained in both modes at a value of 2.8 GHz, and the

nonlinear-mode oscillation amplitude exceeds the linear-mode amplitude by a factor of 17.3.

For the second case, when one of the magnetic resonance frequencies is higher and the other one is lower than the elastic resonance frequency by equal values, the corresponding characteristics are depicted in Fig. 5. Here, due to the different magnetizations of the layers, the magnetic resonance frequency is 3.22 GHz in layer p and 2.38 GHz in layer d. The elastic resonance frequency is 2.8 GHz; i.e., one of the magnetic resonance frequencies is higher and the other one is lower than the elastic resonance frequency by 0.42 GHz.

It is seen from the figure that the linear-mode AFC of magnetic oscillations (see Fig. 5a) have a symmetric bell-shaped form; while, in the nonlinear mode (see Fig. 5b), the vertices of the resonance curves are substantially deflected toward high frequencies, and, as a result, the AFCs acquire triangular shapes. This shape is due to the detuning mechanism [24, 25]. Then, the resonance maximum moves to the frequency 4.35 GHz for layer p and to 3.55 GHz for layer d, i.e., in both cases moves upwards by approximately 1.15 GHz. Thus, the total linear-mode AFC has a double bell-shaped form with two maxima and a deep minimum between them and the total nonlinear-mode AFC has a triangular shape with one characteristic pronounced maximum, a flat low-frequency slope, and a double-step high-frequency slope.

The nonlinear-mode magnetic resonance amplitude increases by a factor of 30.9 (22.7) in layer p (d). The amplitude of total magnetic oscillations at a frequency of 2.8 GHZ increases from 0.125 to 0.85, i.e., by a factor of 68.

The nonlinear-mode AFC for elastic vibrations (see Fig. 5c) for both layers has, besides the main maximum at 2.8 GHz, two additional maxima: near 3.15 (2.4) GHz for layer p (d), a circumstance that characterizes the maxima of excitation at the magnetic resonance frequencies. As a result, the total AFC has a shape of a wide trifolium with three rises at 2.4, 2.9, and 3.2 GHz.

However, in the nonlinear mode (see Fig. 5d), the bell-shaped form of elastic resonances is restored for each layer and for the entire structure and acquires a single maximum near 2.8 GHz. The nonlinear-mode amplitude of total elastic vibrations at 2.8 GHz exceeds the corresponding linear-mode amplitude by a factor of 63.3.

It is interesting to examine the width of the frequency interval of the excited oscillations in both of the considered cases.

Thus, it is seen from Figs. 4a and 4b that, when the frequencies coincide, the half-height-level width of the AFC in the nonlinear-mode for magnetic oscillations (0.5 GHz) exceeds that of the linear-mode ACF (1.5 GHz) by a factor of three. Similarly it is seen from Figs. 5a and 5b that, in the case of different frequencies, the width of the AFC for each of the unit maxima increases from 0.5 to 2.5 GHz, i.e., by a factor of 5, when we pass from the linear to nonlinear mode.

We can see for elastic vibrations from Figs. 4c and 4d that, in the case of coincident frequencies and switching from the linear to nonlinear mode, the AFC width increases from 0.4 to 0.6 GHz, i.e., increases by a factor of 1.5. It is seen from Figs. 5c and 5d that, in the case of different frequencies and switching from the linear to nonlinear mode, the width of the same oscillations decreases from 0.8 to 0.6 GHz, i.e., becomes smaller by the same factor 1.5. Thus, when the frequencies are different, the width of the linear-mode AFC of elastic vibrations exceeds that of the nonlinear-mode AFC by a factor of approximately 2.

At the same time, the nonlinear-mode maximum amplitude of the elastic vibrations excited at the elastic resonance frequency in the cases of equal and different frequencies is about 1.9×10^{-9} cm and the AFC half-height-level width is 0.6 GHz; i.e., the excited elastic vibrations have close parameters for single- and double-layer structures.

Thus, when we pass from a single-layer structure to a double-layer one, the maximum intensity and the width of excited elastic vibrations of the single-layer structure change only slightly. However, the use of a double-layer structure enables one to substantially (no less than by a factor of two) extend the interval of excited frequencies of magnetic oscillations and elastic vibrations.

CONCLUSIONS

The main results of the study are as follows.

The nonlinear problem of hypersound excitation in a normally magnetized double-layer structure has been considered. The elastic properties are constant across the entire thickness, but the magnetic and magnetoelastic properties of the layers can be different. The layers of the structure exhibit cubic anisotropy and magnetostriction.

The equations of motion and boundary conditions for the magnetization components and elastic displacement in both layers have been obtained for the case of an arbitrary angle of the magnetization vector precession. In order to satisfy the inhomogeneous boundary conditions, the original problem is split into two ones: a homogeneous problem with inhomogeneous boundary conditions and an inhomogeneous problem with homogeneous boundary conditions. It has been shown that, as a result of decomposition in the eigenmodes of the entire structure's elastic vibrations, the problem is reduced to a system of the infinite number of second-order differential equations for elastic modes. In the special case when only the first elastic mode is excited, the problem is simplified to a system of 30 nonlinear first-order differential equations (six equations for the layers' magnetizations and 24 equations for the elastic displacements).

The obtained system of equations has been solved numerically with the help of the Runge–Kutta method. The time evolution of oscillations observed as a result of enabling an alternate field has been considered. It has been shown that, in the case of excitation at the elastic resonance frequency when the frequency of the magnetic resonance in one of the layers coincides with the excitation frequency in the linear mode and the frequency of the magnetic resonance in the other layer is below the excitation frequency, the elastic vibrations have a higher amplitude in the layer where the magnetic oscillation frequency coincides with the excitation frequency. In a strongly nonlinear mode, the elastic vibration amplitude in the other layer abruptly grows and exceeds the elastic vibration amplitude in the first layer. As a result, the total amplitude of the excited hypersound substantially increases.

The complicated character of the phase relationships between the excited oscillations and the alternate field has been revealed. Two special cases with simple phase relationships have been indicated. In the first case, the frequencies of both magnetic and elastic resonances coincide; this case is equivalent to a single-layer structure. In the second case, one of the magnetic resonance frequencies is higher and the other one is lower than the elastic resonance frequency by equal values.

The AFCs of the excited oscillations have been investigated for these special cases. The analysis of these characteristics has shown that, when the excitation amplitude increases by two orders of magnitude, the maximum intensity of elastic vibrations excited in a strongly nonlinear mode in both the single- and double-layer structures can exceed the amplitude of the same vibrations in the linear mode by a factor of 30–70. The mutual detuning of the layers' magnetic resonance frequencies enables one to increase the interval of the exited frequencies of both magnetic oscillations and elastic vibrations by a factor of 2–5 as compared to the corresponding frequency interval for the single-layer structure.

ACKNOWLEDGMENTS

This study was supported by the Russian Foundation for Basic Research, project no. 12-02-01035-a.

REFERENCES

1. *Ultrasonic Transducers*, Ed by Y. Kikuchi (Corona Pub. Co., Tokyo, 1969; Mir, Moscow, 1972).
2. I. P. Golyamina, in *Physics and Technology of Powerful Ultrasound,* Vol. 1: *Sources of High-Intensity Ultrasound*, Ed. by L. D. Rozenberg (Nauka, Moscow, 1967) [in Russian].
3. R. L. Comstock and R. C. LeCraw, J. Appl. Phys. **34**, 3022 (1963).
4. R. C. Le Craw and R. L. Comstock, in *Physical Acoustics: Principles and Methods*, Ed. by W. P. Mason (Academic Press, 1964; Mir, Moscow, 1968), Vol. 3B, p. 156.
5. H. E. Bommel and K. Dransfeld, Phys. Rev. Lett. **3** (2), 83 (1959).
6. E. G. Spencer, R. T. Denton, and R. P. Chambers, Phys. Rev. **125**, 1950 (1962).
7. F. G. Eggers and W. Strauss, J. Appl. Phys. **34**, 1180 (1963).
8. *Ferrites in Nonlinear Microwave Hardware* (Inostrannaya Literatura, Moscow, 1961) [in Russian].
9. H. Suhl, J. Phys. Chem. Solids **1** (4), 209 (1957).
10. Ya. A. Monosov, *Nonlinear Ferromagnetic Resonance* (Nauka, Moscow, 1971) [in Russian].
11. V. E. Zakharov, V. S. L'vov, and S. S. Starobinets, Usp. Fiz. Nauk **114**, 609 (1974).
12. A. G. Temiryazev, M. P. Tikhomirova, and P. E. Zilberman, J. Appl. Phys. **76**, 5586 (1994).
13. P. E. Zil'berman, A. G. Temiryazev, and M. P. Tikhomirova, Zh. Eksp. Teor. Fiz. **108** (1), 281 (1995).
14. Yu. V. Gulyaev, P. E. Zil'berman, A. G. Temiryazev, and M. P. Tikhomirova, J. Commun. Technol. Electron. **44**, 1168 (1999).
15. Yu. V. Gulyaev, P. E. Zil'berman, A. G. Temiryazev, and M. P. Tikhomirova, Phys. Solid State **42** (6), 1094 (2000).
16. Th. Gerrits, M. L. Schneider, A. B. Kos, and T. J. Silva, Phys. Rev. **73**, 094454(7) (2006).
17. D. I. Sementsov and A. M. Shutyi, Usp. Fiz. Nauk **177**, 831 (2007).
18. V. S. Vlasov, Candidate's Dissertation in Mathematics and Physics (Mosk. Gos. Univ., Moscow, 2007).
19. S. N. Karpachev, V. S. Vlasov, and L. N. Kotov, Vestn. Mosk. Univ., Ser. 3: Fiz., Astron., No. 6, 60 (2006).
20. V. S. Vlasov, L. N. Kotov, V. G. Shavrov, and V. I. Shcheglov, J. Commun. Technol. Electron. **54**, 821 (2009).
21. V. S. Vlasov, V. G. Shavrov, and V. I. Shcheglov, J. Radioelektron., No. 2 (2013); http://jre.cplire.ru.
22. A. N. Tikhonov and A. A. Samarskii, *Equations of Mathematical Physics* (Nauka, Moscow, 1972; Pergamon Press, Oxford, 1964).
23. G. A. Korn and T. M. Korn, *Mathematical Handbook for Scientists and Engineers: Definitions, Theorems, and Formulas for Reference and Review* (McGraw-Hill, New York, 1961; Nauka, Moscow, 1968).
24. V. V. Migulin, V. I. Medvedev, E. R. Mustel', and V. N. Parygin, *Fundamental Theory of Oscillations* (Nauka, Moscow, 1978) [in Russian].
25. A. G. Gurevich and G. A. Melkov, *Magnetization Oscillations and Waves* (Nauka, Moscow, 1994; CRC, Boca Raton, Fl., 1996).

Translated by I. Efimova